

Article

Combined Experimental and Theoretical Investigation into the Photophysical Properties of Halogenated Coelenteramide Analogs

Ana Carolina P. Afonso ¹, Patricia González-Berdullas ¹, Joaquim C. G. Esteves da Silva ^{1,2}
and Luís Pinto da Silva ^{1,2,*}

¹ Chemistry Research Unit (CIQUP), Institute of Molecular Sciences (IMS), Department of Geosciences, Environment and Territorial Planning, Faculty of Sciences, University of Porto, R. Campo Alegre s/n, 4169-007 Porto, Portugal

² LACOMEPhi, GreenUPorto, Department of Geosciences, Environment and Territorial Planning, Faculty of Sciences, University of Porto, R. Campo Alegre s/n, 4169-007 Porto, Portugal

* Correspondence: luis.silva@fc.up.pt

Abstract: Marine Coelenterazine is one of the most well-known chemi-/bioluminescent systems, and in which reaction the chemi-/bioluminophore (Coelenteramide) is generated and chemiexcited to singlet excited states (leading to light emission). Recent studies have shown that the bromination of compounds associated with the marine Coelenterazine system can provide them with new properties, such as anticancer activity and enhanced emission. Given this, our objective is to characterize the photophysical properties of a previously reported brominated Coelenteramide analog, by employing a combined experimental and theoretical approach. To better analyze the potential halogen effect, we have also synthesized and characterized, for the first time, two new fluorinated and chlorinated Coelenteramide analogs. These compounds show similar emission spectra in aqueous solution, but with different fluorescence quantum yields, in a trend that can be correlated with the heavy-atom effect (F > Cl > Br). A blue shift in emission in other solvents is also verified with the F–Cl–Br trend. More relevantly, the fluorescence quantum yield of the brominated analog is particularly sensitive to changes in solvent, which indicates that this compound has potential use as a microenvironment fluorescence probe. Theoretical calculations indicate that the observed excited state transitions result from local excitations involving the pyrazine ring. The obtained information should be useful for the further exploration of halogenated Coelenteramides and their luminescent properties.

Keywords: chemiluminescence; bioluminescence; Coelenterazine; Coelenteramide; fluorescence; photophysics; microenvironment probe; heavy-atom effect



Citation: Afonso, A.C.P.; González-Berdullas, P.; Esteves da Silva, J.C.G.; Pinto da Silva, L. Combined Experimental and Theoretical Investigation into the Photophysical Properties of Halogenated Coelenteramide Analogs. *Molecules* **2022**, *27*, 8875. <https://doi.org/10.3390/molecules27248875>

Academic Editors: Michael Moustakas, Ilektra Sperdouli and Georgia Ouzounidou

Received: 15 November 2022

Accepted: 10 December 2022

Published: 14 December 2022

Publisher's Note: MDPI stays neutral with regard to jurisdictional claims in published maps and institutional affiliations.



Copyright: © 2022 by the authors. Licensee MDPI, Basel, Switzerland. This article is an open access article distributed under the terms and conditions of the Creative Commons Attribution (CC BY) license (<https://creativecommons.org/licenses/by/4.0/>).

1. Introduction

Chemiluminescence (CL) consists in the emission of radiation due to a chemical reaction [1–4]. A sub-type of CL is bioluminescence (BL), in which light is emitted due to a biochemical reaction (involving an enzyme or photoprotein) [1–4]. BL is widespread in nature and can be found in organisms as different as fireflies, jellyfishes, bacteria, and fungi, among others [1–4]. Typically, light emission from CL/BL reactions originates due to the formation of a high-energy peroxide intermediate, which decomposes rather quickly with high exothermicity, which allows for chemiexcitation to excited states [5–10].

Both CL and BL reactions present a diminished probability for autofluorescence arising from the background signal, which increases the signal-to-noise ratio, as they do not require photoexcitation to generate the chemiexcited light emitter [11,12]. Given this, CL/BL can generate luminescent signals with high sensitivity and almost no background noise [13]. This feature is particularly useful for applications in biologic media, which explains why CL/BL systems have been gaining practical applications in fields such as cancer therapy [14–16], real-time imaging [17–19] and (bio)sensing [20–24].

It should be noted that around 80% of all luminescent organisms are present in the oceans, and most of them employ imidazopyrazinone-based compounds as BL substrates [25], such as Coelenterazine (Clz, Figure 1). In fact, Clz is one of the most well-known and studied compounds among the existing CL and/or BL substrates [26–30]. Interestingly, Clz is capable of both BL (when in the presence of either photoproteins or luciferase enzymes) [2,4] and CL (when in polar aprotic solvents, such as DMF or DMSO, or in the presence of reactive oxygen species, such as superoxide anion) [31–33]. Irrespective of this, CL/BL reactions of Clz occur via the same general mechanism [2,4,26–33]: there is the oxygenation of the imidazopyrazinone core, with the formation of a high-energy peroxide intermediate; this latter compound is highly unstable and undergoes decomposition almost instantly. During this reaction, the reacting molecules can cross to the singlet excited state, thereby generating the chemiexcited light emitter Coelenteramide (Clmd, Figure 1). Clmd is then the species that emits light during both CL and BL reactions and possesses an amidopyrazine core (instead of the imidazopyrazinone core of Clz) [34–36].

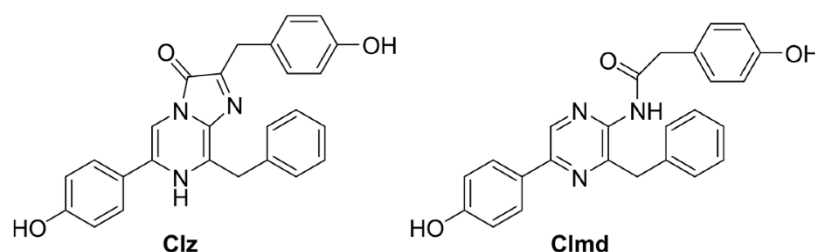


Figure 1. Chemical structures of native Clz and Clmd.

It should be noted that besides developing practical applications for native Clz (and other imidazopyrazinones), the research community has also been active in the development of new molecules based on Clz and with enhanced features, such as red-shifted emission, brighter light emission, and a longer emission half-life [37–40]. Two of the most well-known examples are commercial Coelenterazine 400a (Clz400a) [37,38] and Coelenterazine-e (Clz-e) [41].

Our group has also been active in the development of novel Clz analogs with both enhanced and new properties [42–48]. This effort has had a focus on the introduction of bromine (Br) heteroatoms into the imidazopyrazinone scaffold of Clz (either directly into the core, or by being part of different functional groups). Quite interestingly, this type of modification has provided some novel analogs with quite enhanced CL emission in aqueous solution when compared with native Clz [46–48]. For others, the introduction of Br has provided them with anticancer activity toward different cancer cell types (prostate, breast, neuroblastoma, lung, and/or gastric cancer). Thus, it is clear that bromination is a relevant strategy in modifying Clz.

Among the developed analogs, we highlight one in which the phenol, benzyl, and *p*-cresol moieties of Clz (Figure 1) are replaced by a bromophenyl moiety, a hydrogen atom, and a methyl group (Br-Clz, Figure 2), respectively [43–45]. This compound presents cytotoxicity toward both prostate and breast cancer (IC₅₀ of 24.28 and 21.56 μM, respectively), while analysis with non-cancer cells demonstrated a relevant profile of tumor selectivity [43,44]. Quite interestingly, we have found that its corresponding Clmd version (Br-Clmd, Figure 2) also presents anticancer activity, albeit apparently not by the same mode of action [45]. More specifically, Br-Clmd showed activity toward both gastric and lung cancer (IC₅₀ of 16.2 and 10.1 μM, respectively) [45]. Given this, it does appear that the modification of Clmd with the inclusion of Br heteroatoms is also a good strategy to tune the properties of this species.

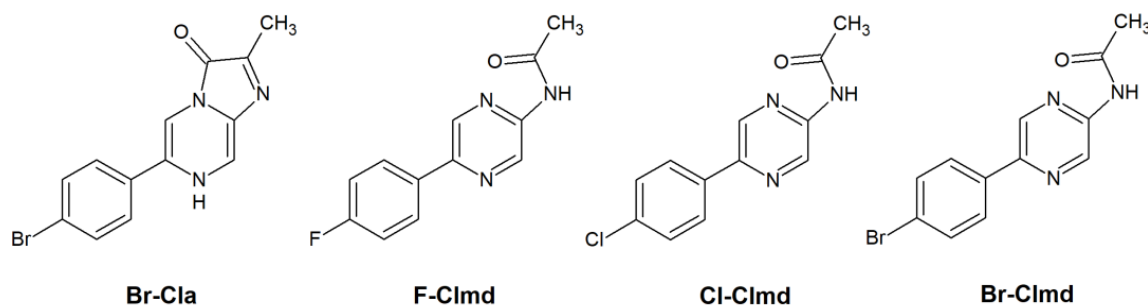


Figure 2. Chemical structures of the halogenated Br-Cla and Clmds (F-, Cl-, and Br-Clmd).

Thus, given the previous information and the role of Clmd as a light emitter in CL/BL reactions [34–36], the aim of this work is then to evaluate, for the first time, the photophysical properties of Br-Clmd (Figure 2) by employing a combined experimental and theoretical approach. With this study, we intend to assess whether bromination is a relevant strategy to improve/modify the luminescent properties of Clmd-based compounds. To further evaluate whether changes are indeed due to Br, and not due to more general halogen-based effects, we have also synthesized and studied two novel Clmd analogs: F- and Cl-Clmd (Figure 2). The data obtained in this study should be useful for researchers focused on the development of Clz/Clmd-based systems with enhanced/new features.

2. Results and Discussion

2.1. Photophysical Characterization of the Clmd Analogs

The absorption spectra of the three halogenated Clmd analogs, in aqueous solution, are presented in Figure 3. The three analogs present spectra with a very similar shape and peak position. This is particularly true for Cl- and Br-Clmd, whose spectra are composed of two peaks at ~270 and ~320 nm, with identical relative intensities between them. The absorption spectrum of F-Clmd is also similar, as it is composed of two peaks, with one of them with a maximum also at ~320 nm. However, the other peak is slightly blue-shifted (~260 nm). Moreover, it appears that the relative difference in intensity between the peaks for F-Clmd is not the same as for Cl-/Br-Clmd. Compared with the literature [36,49], the absorption of all halogenated compounds (red-shifted peak at ~320) is blue-shifted relative to native Clmd (335–340 nm).

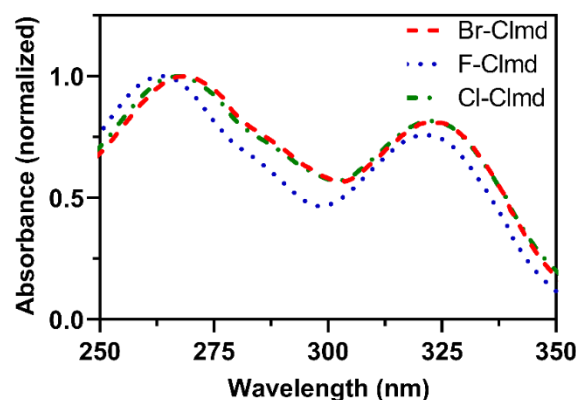


Figure 3. UV-Vis spectra of the halogenated Clmds in aqueous solution.

The fluorescence spectra of the compounds were obtained in different solvents (Figure 4): deionized water, dimethyl sulfoxide (DMSO), and methanol (MeOH). These solvents are typically used in the study of the CL/BL system of Clz/Clmd [12,27,28,31–33,35,46,47].

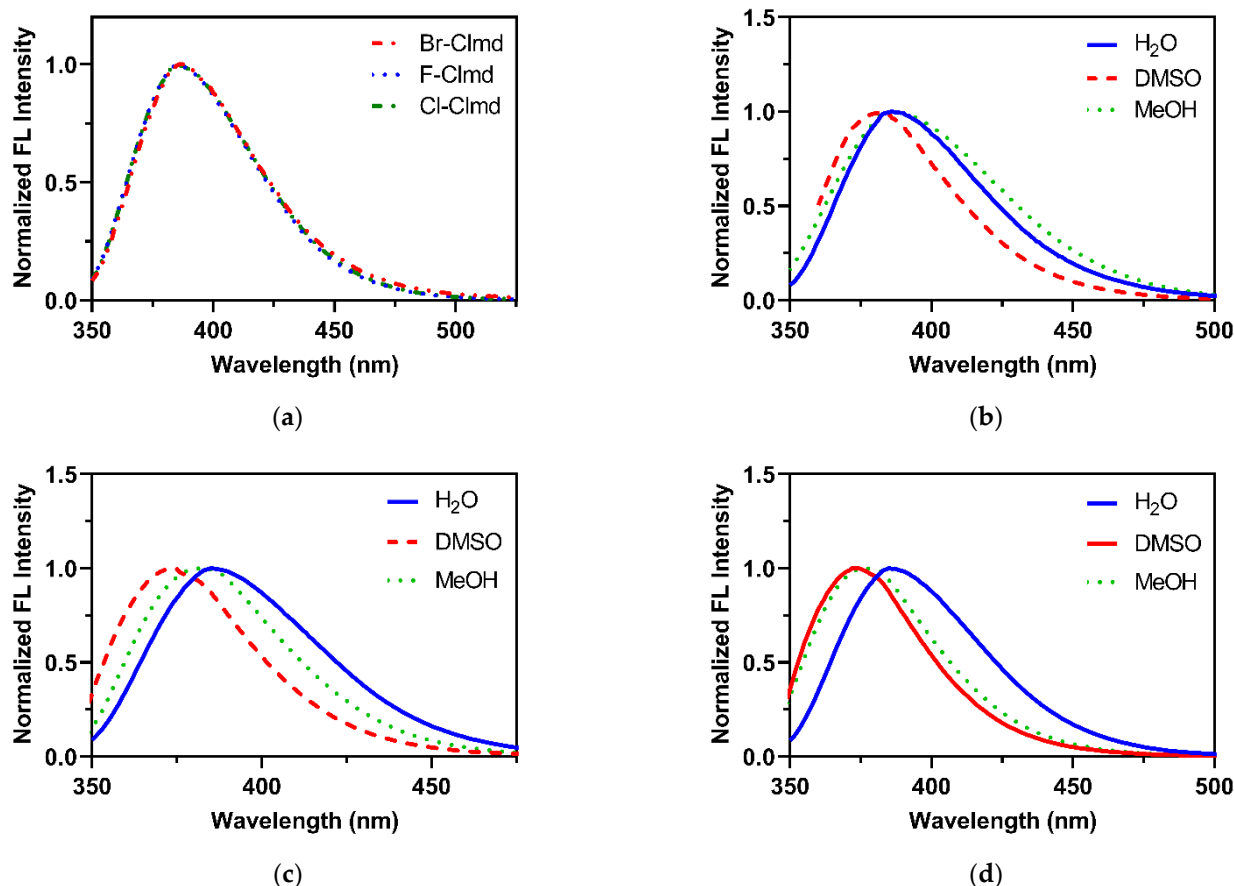


Figure 4. Normalized fluorescence (FL) spectra for the compounds studied in different solvents. (a) Halogenated Clmds in deionized water; (b) Br-Clmd; (c) F-Clmd; (d) Cl-Clmd. Excitation at 310 nm.

In an aqueous solution (Figure 4a), the three halogenated compounds present overlapped spectra, with an emission maximum at 385 nm. Thus, in aqueous solution, varying the halogen heteroatom does not affect the shape of the fluorescence spectra of these compounds. This emission maximum is in line with the emission typically attributed to the neutral form of native Clmd, which emits from 386 to 391 nm in benzene [49] and up to 420 nm in MeOH [35]. This information helps us to attribute the emitted fluorescence to the neutral form (Figure 2) of F-/Cl-/Br-Clmd.

The measurement of fluorescence in other solvents (Figure 4) indicates that the more red-shifted emission is found in water, while the more blue-shifted emission was measured in DMSO for all compounds (by 10 nm). Interestingly, the main difference between the compounds is their fluorescence in MeOH. For Br-Clmd, there is an overlap between the emission spectra in aqueous solution and in MeOH. However, for Cl-Clmd, there is a ~5 nm blue shift between the emission in water and in MeOH. This blue shift further increases to ~8 nm for F-Clmd. Thus, there does appear to exist a halogen-dependent effect regarding the emission of the compounds in MeOH.

Finally, given the highest emission wavelength for these compounds (385 nm) and the emission maxima previously reported for native Clmd (up to 420 nm [35,49]), it is clear that the emission of these Clmd analogs is more blue-shifted than for the natural compound.

2.2. Fluorescence Quantum Yield

The QY values for the three studied compounds, in the studied solvents, are presented in Table 1. There is great variability for the three compounds in the aqueous solution, as the QY values range from 8 to 26%. Interestingly, we can see that the QY (in water) increases

from the heaviest halogen to the lightest one: Br (8%) < Cl (23%) < F (26%). This could be attributed to the heavy-atom effect [50], as it can reduce QY by enhancing intersystem crossing (ISC) to triplet states [44,50]. In fact, the introduction of Br heteroatoms is a typical strategy to enhance ISC, due to the heavy-atom effect, which correlates well with the obtained results in aqueous solution.

Table 1. Fluorescence quantum yields (QY, in %) in different solvents.

	Br-Clmd	Cl-Clmd	F-Clmd
Water	8%	23%	26%
DMSO	14%	14%	12%
MeOH	17%	18%	15%

However, this halogen-dependent effect was no longer observed in DMSO, as the QY values were similar for all three compounds. It should be noted, nevertheless, that this similarity results from a relevant decrease in yield (from 23–26% to 12–14%) for F-/Cl-Clmd, and an increase for Br-Clmd (from 8 to 14%). In MeOH, there is an even higher increase to 17%, regarding its yield in an aqueous solution. For F-/Cl-Clmd, their QY values in MeOH were higher than in DMSO, but lower than in water. For these organic solvents, there is not a particularly noticeable heavy-atom effect, as the highest QY was observed for Cl-Clmd, followed by Br-Clmd and then by F-Clmd.

In short, there is an indication that the heavy-atom effect plays a role in the QY of the halogenated Clmd analogs in aqueous solution. However, in other solvents, other factors besides the heavy-atom effect should have a greater role on the obtained QY values. Nevertheless, if the reduced QY values in aqueous solutions (closer to biological media) are indeed due to the heavy-atom effect, this could mean that Br-Clmd could have intrinsic value as the basis for a photosensitizer [50].

2.3. Fluorescence Response to Variations in Solution

There is an increasing focus among the research community to develop fluorescent probes for microenvironment-related parameters (such as polarity, viscosity, and pH) [51–53]. These play important roles in the control of the physical–chemical behaviors of local molecules [51–53]. Thus, such probes can be very useful in the study of both physiological and pathological processes [51–53].

As can be seen in both Table 1 and Figure 4, while the emission wavelength of Br-Clmd is not particularly affected by the microenvironment, this is not the case regarding its QY. Thus, it is possible that this molecule could have potential to be used as a fluorescent probe for the local microenvironment by measuring the variation in its fluorescent intensity. To better assess this, we then measured the fluorescence intensity (F/F_0) of a 10 μ M solution of Br-Clmd with an increasing ratio of MeOH in water (from 0 to 100%, with increments of 25%). The results can be found in Figure 5. We did observe a gradual increase in fluorescence with an increasing ratio of MeOH in the solution, reaching an approximately 2.5 times increase in pure MeOH and almost two times in 25%/75% water/MeOH. Thus, the fluorescence of Br-Clmd is indeed affected by changes in the microenvironment. Given this, this type of compound has potential to be further explored as a basis for new probes for microenvironment-related parameters. Regarding the reason that this change in fluorescence intensity occurs, it should be noted that it has been previously reported that water can act as a fluorescence quencher [54–56]. In fact, different fluorophores have been found to present lower QY values in water than in organic solvents [55,56]. Therefore, the quenching effect of water can help to explain the intensity variation here observed. Nevertheless, further research should be performed in the future to better understand this phenomenon.

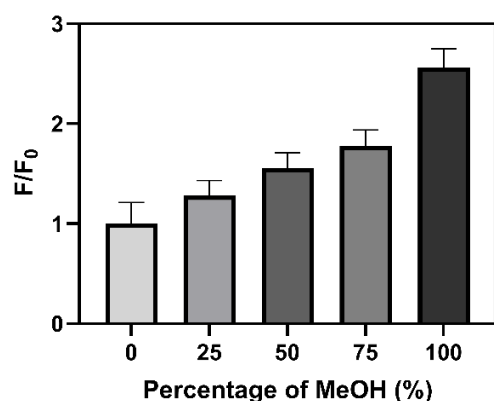


Figure 5. Variation in Br-Clmd fluorescence intensity (F/F_0) in mixtures of water and MeOH (from 0 to 100%).

2.4. Theoretical Investigation of the Photophysics of Br-Clmd

To obtain further information about the photophysics of Br-Clmd, we attempted to characterize the electron excitation of this molecule in implicit water (with a vertical approximation) by using hole–electron analysis [57]. This was performed at the TD-DFT level of theory, with three different density functionals: ω B97XD, CAM-B3LYP, and PBE0. We focused on the neutral species of Br-Clmd, given the match between the photophysical properties here measured with those of native Clmd [35,49]. Furthermore, Br-Clmd can potentially coexist in one of two conformations (Br-Clmd-1 and Br-Clmd-2), as seen in Figure 6. The latter one was found to be more stable than the former by 4.2 kcal mol^{−1} (Gibbs free energy with thermal corrections), and so we focused on Br-Clmd-2 in the subsequent analysis.

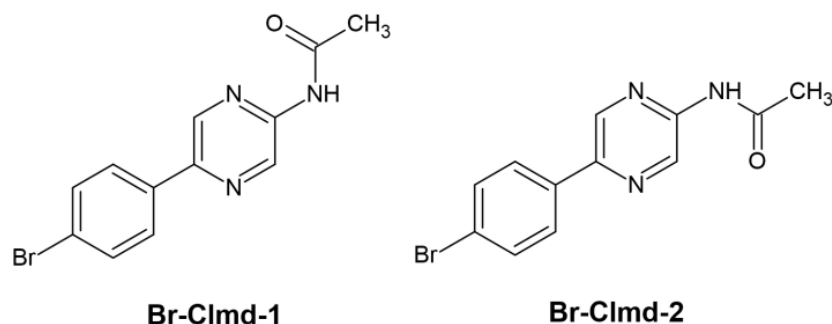


Figure 6. Possible conformations for Br-Clmd.

In Table 2, we present the excitation wavelength (λ_{ex} , in nm), the oscillator strength (f), and the S_r index for the $S_0 \rightarrow S_1$ vertical excitation of Br-Clmd-2, as calculated with the three density functionals: ω B97XD, CAM-B3LYP, and PBE0. The S_r index characterizes the overlapping extent of holes and electrons (its theoretical upper limit being 1.0) [57]. While PBE0 does provide λ_{ex} values close to the experimentally determined ones (Figure 3), ω B97XD and CAM-B3LYP do not appear to reproduce experiment well. Nevertheless, all agree on the value for the S_r index: 0.745–0.772. It should be remembered that this index evaluates the overlapping extent of hole and electron distribution (upon electron excitation) and possesses a theoretical upper limit of 1.0 [57]. This indicates that more than half of the hole and electron are perfectly matched [57]. Thus, we can attribute this $S_0 \rightarrow S_1$ transition to the LE type.

Table 2. Excitation wavelength (λ_{ex} , in nm), oscillator strength (f), and S_r index for the $S_0 \rightarrow S_1$ excitation of Br-Clmd-2 in implicit water, when calculated at the TD-DFT level of theory with different functionals.

Density Functionals	λ_{ex}	f	S_r
ω B97XD	286	0.71	0.772
CAM-B3LYP	288	0.72	0.769
PBE0	305	0.67	0.745

It was also found that the $S_0 \rightarrow S_1$ transition corresponds to a HOMO \rightarrow LUMO excitation (Figure 7). More specifically, the studied transition appears to be a $\pi \rightarrow \pi^*$ local excitation (LE), with a relevant overlap of hole and electron in the pyrazine ring.

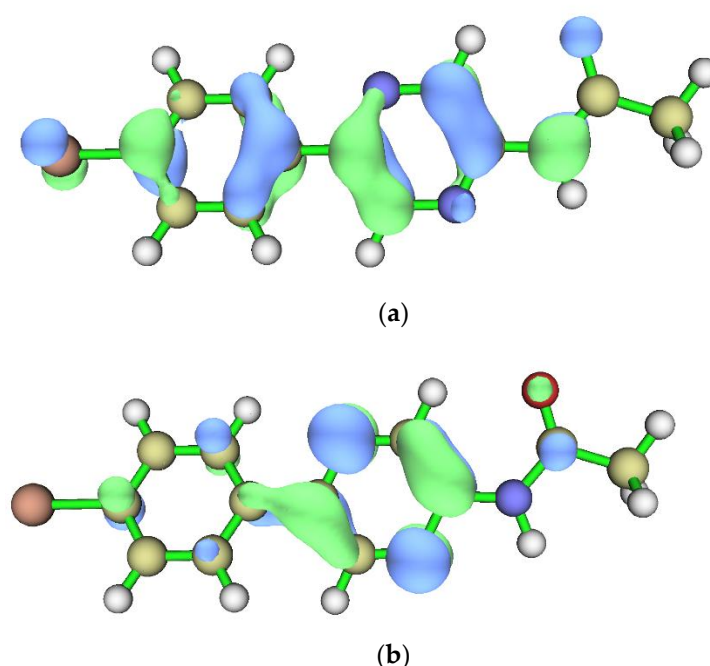


Figure 7. HOMO (a) and LUMO (b) orbitals for Br-Clmd-2 in implicit water, when calculated at the TD-PBE0 level of theory.

3. Materials and Methods

3.1. Synthesis of Halogenated Clmds

The synthesis of the studied compounds started with the functionalization of commercial 5-bromopyrazin-2-amine, via a Suzuki–Miyaura cross-coupling reaction with commercial boronic acids (with procedures described in more detail in the Supplementary Materials). This yielded the corresponding F-, Cl-, and Br-substituted phenylpyrazin-2-amine (Coelenteramine, Clm) synthesis intermediates, which were already described in [43–45,47]. The final Clmd structures were obtained for all three compounds through N-acetylation of the Clm intermediates, by using pyridine as the base to avoid the formation of the disubstituted subproduct. The structural characterization was performed by using both ^1H - and ^{13}C -NMR spectroscopy, as well as FT-MS spectrometry. Br-Clmd have already been described in the literature [45], while further details for F- and Cl-Clmd can be found in the Supplementary Materials (Figures S1–S4).

3.2. Photophysical Characterization

The fluorescence spectra were analyzed via fluorescence spectroscopy, using a standard 10 mm quartz cuvette, with a Horiba Yvon Fluoromax-4 fluorimeter [58]. The emission and excitation spectra were obtained with a 1 nm capture interval and 2 nm slit

width. Absorption spectra were obtained with a VWRs UV-3100PC spectrophotometer, by using quartz cells. Assays were performed with a concentration of 10 μM of the studied compounds.

3.3. Determination of the Fluorescence Quantum Yield

The fluorescence quantum yield (QY) was calculated by comparing the integrated luminescence intensities and the absorbance values of the compounds with the following equation:

$$QY = QY_R \times \frac{Grad}{Grad_R} \times \frac{\eta^2}{\eta_R^2} \quad (1)$$

In the equation, QY is the fluorescence quantum yield, *Grad* is the gradient from the plot of integrated fluorescence intensity versus absorbance, and η is the refractive index. The subscript *R* refers to the reference fluorophore with a known QY. In this work, quinine sulfate in 0.1 M H_2SO_4 was used, with a QY of 54% [59]. Quinine sulfate was the fluorescence standard selected as it has a similar excitation wavelength and emission spectrum to the studied compounds [59]. The refractive index is 1.33 for aqueous solutions, 1.326 for methanol, and 1.479 for DMSO [60–62].

3.4. Theoretical Calculations

The geometry optimizations for the singlet ground state (S_0) of the studied molecules were performed with the ωB97XD density functional [63]. A 6-31G(d,p) basis set was used for H, C, N, and O, while the LANL2DZ basis set was used for Br. Frequency calculations were performed at the same level of theory. The S_0 energies were re-evaluated using single-point calculations with the same functional as before, while increasing the basis sets: 6-31+G(d,p) for H, C, N, and O, and LANL2DZ with polarization and diffuse functions for Br. The vertical excitations to singlet excited states were calculated at the TD- ωB97XD level of theory, with the previously mentioned basis sets. ωB97XD was chosen as it generally provides accurate estimates for $\pi \rightarrow \pi^*$ and $n \rightarrow \pi^*$ LE, charge transfer, and Rydberg states [64]. To limit density-functional-related errors, vertical excitations were also calculated with other functionals: CAM-B3LYP [65] and PBE0 [66]. All calculations were performed in an implicit solvent, by using a polarizable continuum model (IEFPCM). These calculations were performed by using the Gaussian 09 program package [67].

The electron excitation analysis was performed with the MultiWFN software [57], based on the Gaussian-09-based calculations. More specifically, the quantitative characterization of the hole and electron distribution (upon electron excitation) was performed by calculating the S_r index, which characterizes the overlapping extent of holes and electrons (its theoretical upper limit being 1.0) [57].

4. Conclusions

In this study, we investigated the photophysical properties of three halogenated Clmd analogs: F-Clmd, Cl-Clmd, and Br-Clmd. This investigation was performed with a combined experimental and theoretical approach. The measured UV-Vis and fluorescence spectra of the compounds were quite similar in aqueous solution, with absorption and emission at ~ 320 and 385 nm, respectively. These data indicate that the luminescence of the halogenated analogs is blue-shifted with respect to native Clmd. Interestingly, the emission of the analogs is blue-shifted in organic solvents, whose magnitude is related to the F-Cl-Br trend. Furthermore, the fluorescence quantum yield of the analogs in aqueous solution increases in the order of $\text{Br} < \text{Cl} < \text{F}$, which can be correlated with the heavy-atom effect (and possible enhancement of intersystem crossing). Of additional relevance is the fact that while the emission spectra of Br-Clmd is similar in different solvents, its fluorescence quantum yield changes significantly. In fact, changing the water/methanol ratio of mixtures led to an increase in the fluorescence intensity of this compound by around 2.5 times. Thus, this analog shows some potential for use as the basis for the development of a fluorescence probe to detect changes in the local microenvironment. Theoretical calculations at the

TD-DFT level indicated that the excited state transitions here observed are local excitations involving mainly the pyrazine ring of Clmd species.

Supplementary Materials: The following supporting information can be downloaded at: <https://www.mdpi.com/article/10.3390/molecules27248875/s1>, Figure S1: ¹H-NMR, ¹³C-NMR and DEPT spectra of *N*-(5-(4-fluorophenyl)pyrazine-2-yl)acetamide (F-Clmd). Figure S2: ¹H-NMR, ¹³C-NMR and DEPT spectra of *N*-(5-(4-chlorophenyl)pyrazin-2-yl)acetamide (Cl-Clmd). Figure S3: FTMS-ESI (+) spectrum of *N*-(5-(4-fluorophenyl)pyrazin-2-yl)acetamide (F-Clmd). Figure S4: FTMS-ESI (+) spectrum of *N*-(5-(4-chlorophenyl)pyrazin-2-yl)acetamide (Cl-Clmd).

Author Contributions: Conceptualization, L.P.d.S.; investigation, A.C.P.A., P.G.-B. and L.P.d.S.; writing—original draft preparation, A.C.P.A. and P.G.-B.; writing—review and editing, L.P.d.S. and J.C.G.E.d.S.; supervision, L.P.d.S.; funding acquisition, L.P.d.S. All authors have read and agreed to the published version of the manuscript.

Funding: The Portuguese “*Fundação para a Ciência e Tecnologia*” (FCT, Lisbon) is acknowledged for funding project PTDC/QUI-QFI/2870/2020, the R&D Units CIQUP (UIDB/00081/2020), GreenUPorto (UIDB/05748/2020), and the Associated Laboratory IMS (LA/P/0056/2020). Luís Pinto da Silva acknowledges funding from FCT under the Scientific Employment Stimulus (CEECINST/00069/2021). Patricia González-Berdullas acknowledges project PTDC/QUI-QUI/2870 for funding her postdoctoral position. Ana Carolina P. Afonso acknowledges FCT for her Ph.D. grant (2022.13031.BD).

Acknowledgments: The Laboratory of Computational Modelling of Environmental Pollutant-Human Interactions (LACOMEPhi) and the Materials Centre of the University of Porto (CEMUP) are acknowledged.

Conflicts of Interest: The authors declare no conflict of interest.

References

1. Magalhães, C.M.; Esteves da Silva, J.C.G.; Pinto da Silva, L. Chemiluminescence and bioluminescence as an excitation source in the photodynamic therapy of cancer: A critical review. *Chem. Phys. Chem.* **2016**, *17*, 2286–2294. [[CrossRef](#)] [[PubMed](#)]
2. Vacher, M.; Galván, I.F.; Ding, B.W.; Schramm, S.; Berraud-Pache, R.; Naumov, P.; Ferré, N.; Liu, Y.J.; Navizet, I.; Roca-Sanjuán, D.; et al. Chemi- and bioluminescence of cyclic peroxides. *Chem. Rev.* **2018**, *118*, 6927–6974. [[CrossRef](#)]
3. Carrasco-López, C.; Lui, N.M.; Schramm, S.; Naumov, P. The elusive relationship between structure and colour emission in beetle luciferases. *Nat. Rev. Chem.* **2021**, *5*, 4–20. [[CrossRef](#)]
4. Kaskova, Z.M.; Tsarkova, A.S.; Yampolsky, I.V. 1001 lights: Luciferins, luciferases, their mechanisms of action and applications in chemical analysis, biology and medicine. *Chem. Soc. Rev.* **2016**, *45*, 6048–6077. [[CrossRef](#)] [[PubMed](#)]
5. Boara, A.; Reis, R.A.; Silva, C.S.; Melo, D.U.; Pinto, A.G.G.C.; Bartoloni, F.H. Evidence for the formation of 1,2-dioxetane as a high-energy intermediate and possible chemiexcitation pathways in the chemiluminescence of lophine peroxides. *J. Org. Chem.* **2021**, *86*, 6633–6647. [[CrossRef](#)] [[PubMed](#)]
6. Schramm, S.; Navizet, I.; Karothu, S.P.; Oeasu, P.; Bensmann, V.; Weiss, D.; Beckert, R.; Naumov, P. Mechanistic Investigations of the 2-coumarone chemiluminescence. *Phys. Chem. Chem. Phys.* **2017**, *19*, 22852–22859. [[CrossRef](#)]
7. Khalid, M.; Sousa, S.P., Jr.; Cabello, M.C.; Bartoloni, F.H.; Ciscato, L.F.M.L.; Bastos, E.L.; El Seoud, O.A.; Baader, W.J. Solvent polarity influence on chemiexcitation efficiency of inter and intramolecular electron-transfer catalyzed chemiluminescence. *J. Photochem. Photobiol. A* **2022**, *433*, 114161. [[CrossRef](#)]
8. Magalhães, C.M.; Esteves da Silva, J.C.G.; Pinto da Silva, L. Tuning the Intramolecular Chemiexcitation of Neutral Dioxetanones by Interaction with Ionic Species. *Molecules* **2022**, *27*, 3861. [[CrossRef](#)]
9. Magalhães, C.M.; Esteves da Silva, J.C.G.; Pinto da Silva, L. Theoretical Study of Thermolysis Reaction and Chemiexcitation of Coelenterazine Dioxetanones. *J. Phys. Chem. A* **2022**, *126*, 3486. [[CrossRef](#)]
10. Pinto da Silva, L.; Magalhães, C.M.; Esteves da Silva, J.C.G. Interstate Crossing-Induced Chemiexcitation Mechanism as the Basis for Imidazopyrazinone Bioluminescence. *ChemistrySelect* **2016**, *1*, 3343–3356. [[CrossRef](#)]
11. Gnaïm, S.; Shabat, D. Self-Immolative Chemiluminescence Polymers: Innate Assimilation of Chemiexcitation in a Domino-Like Depolymerization. *J. Am. Chem. Soc.* **2017**, *139*, 10002–10008. [[CrossRef](#)] [[PubMed](#)]
12. Pinto da Silva, L.; Pereira, R.F.J.; Magalhães, C.M.; Esteves da Silva, J.C.G. Mechanistic Insight into Cypridina Bioluminescence with a Combined Experimental and Theoretical Chemiluminescent Approach. *J. Phys. Chem. B* **2017**, *121*, 7862–7871. [[CrossRef](#)] [[PubMed](#)]
13. Yang, M.; Huang, J.; Fan, J.; Du, J.; Pu, K.; Peng, X. Chemiluminescence for bioimaging and therapeutics: Recent advances and challenges. *Chem. Soc. Rev.* **2020**, *49*, 6800–6815. [[CrossRef](#)] [[PubMed](#)]
14. Jiang, L.; Bai, H.; Liu, L.; Lv, F.; Ren, X.; Wang, S. Luminescent, Oxygen-Supplying, Hemoglobin-Linked Conjugated Polymer Nanoparticles for Photodynamic Therapy. *Angew. Chem. Int. Ed.* **2019**, *58*, 10660–10665. [[CrossRef](#)]

15. Gao, J.; Chen, Z.; Li, X.; Yang, M.; Lv, J.; Li, H.; Yuan, Z. Chemiluminescence in Combination with Organic Photosensitizers: Beyond the Light Penetration Depth Limit of Photodynamic Therapy. *Int. J. Mol. Sci.* **2022**, *23*, 12556. [[CrossRef](#)]
16. Blum, N.T.; Zhang, Y.; Qu, J.; Lin, J.; Huang, P. Recent Advances in Self-Exciting Photodynamic Therapy. *Front. Bioeng. Biotechnol.* **2020**, *8*, 894491. [[CrossRef](#)]
17. Cronin, M.; Akin, A.R.; Francis, K.P.; Tangney, M. In vivo bioluminescence imaging of intratumoral bacteria. *Methods Mol. Biol.* **2016**, *1409*, 69–77.
18. Grinstead, K.M.; Rowe, L.; Ensor, C.M.; Joel, S.; Daftarian, P.; Dikici, E.; Zingg, J.M.; Daunert, S. Red-Shifted Aequorin Variants Incorporating Non-Canonical Amino Acids: Applications in in vivo Imaging. *PLoS ONE* **2016**, *11*, e0158579. [[CrossRef](#)]
19. Zhang, Y.; Pang, L.; Ma, C.; Tu, Q.; Zhang, R.; Saeed, E.; Mahmoud, A.E.; Wang, J. Small Molecule-Initiated Light-Activated Semiconducting Polymer Dots: An Integrated Nanoplatfor for Targeted Photodynamic Therapu and Imaging of Cancer Cells. *Anal. Chem.* **2014**, *86*, 3092–3099. [[CrossRef](#)]
20. Ievtukhov, V.; Zadykovicz, B.; Blazheyevsky, M.Y.; Krzyminski, K. New luminometric method for quantification of biological sulfur nucleophiles with the participation of 9-cyano-10-methylacridinium salt. *Luminescence* **2022**, *37*, 208–219. [[CrossRef](#)]
21. Berneschi, S.; Trono, C.; Mirasoli, M.; Giannetti, A.; Zangheri, M.; Guardigli, M.; Tombelli, S.; Marchigiani, E.; Baldini, F.; Roda, A. In-Parallel Polar Monitoring of Chemiluminescence Emission Anisotropy at the Solid-Liquid Interface by an Optical Fiber Radial Array. *Chemosensors* **2020**, *8*, 18. [[CrossRef](#)]
22. Krzyminski, K.K.; Roshal, A.D.; Rudnicki-Velasquez, P.B.; Zamojc, K. On the use of acridinium indicators for the chemiluminescent determination of the total antioxidant capacity of dietary supplements. *Luminescence* **2019**, *34*, 512–519. [[CrossRef](#)] [[PubMed](#)]
23. Krasiskaya, V.V.; Bachmakova, E.E.; Frank, L.A. Coelenterazine-dependent luciferases as a powerful analytical tool for research and biomedical applications. *Int. J. Mol. Sci.* **2020**, *21*, 7465. [[CrossRef](#)] [[PubMed](#)]
24. Shelef, O.; Sedgwick, A.C.; Pozzi, S.; Green, O.; Satchi-Fainaro, R.; Shabat, D.; Sesslet, J.L. Turn on chemiluminescence-based probes for monitoring tyrosinase activity in conjunction with biological thiols. *Chem. Commun.* **2021**, *57*, 11386–11389. [[CrossRef](#)]
25. Haddock, S.H.D.; Moline, M.A.; Case, J.F. Bioluminescence in the sea. *Annu. Rev. Mar. Sci.* **2010**, *2*, 443–493. [[CrossRef](#)]
26. Jiang, T.; Du, L.; Li, M. Lighting up bioluminescence with coelenterazine: Strategies and applications. *Photochem. Photobiol. Sci.* **2016**, *15*, 466–480. [[CrossRef](#)]
27. Lourenço, J.M.; Esteves da Silva, J.C.G.; Pinto da Silva, L. Combined experimental and theoretical study of Coelenterazine chemiluminescence in aqueous solution. *J. Lumin.* **2018**, *194*, 139–145. [[CrossRef](#)]
28. Teranishi, K. Luminescence of imidazo,2-a]pyrazin-3(7H)-one compounds. *Bioorg. Chem.* **2007**, *35*, 82–111. [[CrossRef](#)]
29. Magalhães, C.M.; Esteves da Silva, J.C.G.; Pinto da Silva, L. Study of coelenterazine luminescence: Electrostatic interactions as the controlling factor for efficient chemiexcitation. *J. Lumin.* **2018**, *199*, 339–347. [[CrossRef](#)]
30. Buralova, L.P.; Lyakhovich, M.S.; Mineev, K.S.; Petushkov, V.N.; Zagitova, R.I.; Tsarkova, A.S.; Kovalchuk, S.I.; Yampolsky, I.V.; Vysotcki, E.S.; Kaskova, Z.M. Unexpected coelenterazine degradation products of beroe abyssicola photoprotein photoinactivation. *Org. Lett.* **2021**, *23*, 6846–6849. [[CrossRef](#)]
31. Teranishi, K. Non-invasive and accurate readout of superoxide anion in biological systems by near-infrared light. *Anal. Chim. Acta* **2021**, *1179*, 338827. [[CrossRef](#)] [[PubMed](#)]
32. Bronsart, L.L.; Stokes, C.; Contag, C.H. Multimodality imaging of cancer superoxide anion using the small molecular coelenterazine. *Mol. Imaging Biol.* **2016**, *18*, 166–171. [[CrossRef](#)] [[PubMed](#)]
33. Goto, T.; Takgi, T. Chemiluminescence of a Cypridina luciferin analogue, 2-methyl-6-phenyl-3,7-dihydroimidazo(1,2-a)pyrazin-3-one, in the presence of the xanthine-xanthine oxidase system. *Bull. Chem. Soc. Jpn.* **1980**, *53*, 833–834. [[CrossRef](#)]
34. Min, C.G.; Pinto da Silva, L.; Esteves da Silva, J.C.G.; Yang, X.K.; Huang, S.J.; Ren, A.M.; Zhu, Y.Q. A computational investigation of the equilibrium constants for the fluorescent and chemiluminescent states of coelenteramide. *Chem. Phys. Chem.* **2017**, *18*, 117–123. [[CrossRef](#)] [[PubMed](#)]
35. Alieva, R.R.; Tomilin, F.N.; Kuzubov, A.A.; Ovchinnikov, S.G.; Kudryasheva, N.S. Ultraviolet fluorescence of coelenteramide and coelenteramide-containing fluorescent proteins. Experimental and theoretical study. *J. Photochem. Photobiol. B* **2016**, *162*, 318–323. [[CrossRef](#)]
36. Min, C.G.; Li, Z.S.; Ren, A.M.; Zou, L.; Guo, J.; Goddard, J.D. The fluorescent properties of coelenteramide, a substrate of aequorin and obelin. *J. Photochem. Photobiol. A* **2013**, *251*, 182–188. [[CrossRef](#)]
37. Li, J.; Wang, X.; Dong, G.; Yan, C.; Cui, Y.; Zhang, Z.; Du, L.; Li, M. Novel furimazine derivatives for nanoluciferase bioluminescence with various C-6 and C-8 substituents. *Org. Biomol. Chem.* **2021**, *19*, 7930. [[CrossRef](#)]
38. Yuan, M.L.; Jiang, T.Y.; Du, L.P.; Li, M.Y. Luminescence of coelenterazine derivatives with C-8 extended electronic conjugation. *Chin. Chem. Lett.* **2016**, *27*, 550–554. [[CrossRef](#)]
39. Gagnot, G.; Hervin, V.; Coutant, E.P.; Goyard, S.; Jacob, Y.; Rose, T.; Hibti, F.E.; Quatela, A.; Janin, Y.L. Core-Modified Coelenterazine Luciferin Analogues: Synthesis and Chemiluminescence Properties. *Chem. Eur. J.* **2021**, *27*, 2112–2123. [[CrossRef](#)]
40. Jiang, T.; Yang, X.; Zhou, Y.; Yampolsky, I.; Du, L.; Li, M. New bioluminescent coelenterazine derivatives with various C-6 substitutions. *Org. Biomol. Chem.* **2017**, *15*, 7008. [[CrossRef](#)]
41. Shimomura, O.; Musicki, B.; Kishi, Y. Semi-synthetic aequorins with improved sensitivity to Ca²⁺ ions. *Biochem. J.* **1989**, *261*, 913–920. [[CrossRef](#)] [[PubMed](#)]

42. Pinto da Silva, L.; Magalhães, C.M.; Núñez-Montenegro, A.; Ferreira, P.J.O.; Duarte, D.; Rodríguez-Borges, J.E.; Vale, N.; Da Silva, J.C.G.E. Study of the combination of self-activating photodynamic therapy and chemotherapy for cancer treatment. *Biomolecules* **2019**, *9*, 384. [[CrossRef](#)] [[PubMed](#)]
43. Pinto da Silva, L.; Núñez-Montenegro, A.; Magalhães, C.M.; Ferreira, P.J.O.; Duarte, D.; González-Berdullas, P.; Rodríguez-Borges, J.E.; Vale, N.; da Silva, J.C.G.E. Single-molecule chemiluminescent photosensitizer for a self-activating and tumor-selective photodynamic therapy of cancer. *Eur. J. Med. Chem.* **2019**, *183*, 11683. [[CrossRef](#)] [[PubMed](#)]
44. Magalhães, C.M.; González-Berdullas, P.; Duarte, D.; Correia, A.S.; Rodríguez-Borges, J.E.; Vale, N.; Esteves da Silva, J.C.G.; Pinto da Silva, L. Target-Oriented Synthesis of Marine Coelenterazine Derivatives with Anticancer Activity by Applying the Heavy-Atom Effect. *Biomedicines* **2021**, *9*, 1199. [[CrossRef](#)] [[PubMed](#)]
45. González-Berdullas, P.; Pereira, R.B.; Teixeira, C.; Silva, J.P.; Magalhães, C.M.; Rodríguez-Borges, J.E.; Pereira, D.M.; Esteves da Silva, J.C.G.; Pinto da Silva, L. Discovery of the Anticancer Activity for Lung and Gastric Cancer of a Brominated Coelenteramine Analog. *Int. J. Mol. Sci.* **2022**, *23*, 8271. [[CrossRef](#)] [[PubMed](#)]
46. Silva, J.P.; González-Berdullas, P.; Esteves da Silva, J.C.G.; Pinto da Silva, L. Development of a Coelenterazine Derivative with Enhanced Superoxide Anion-Triggered Chemiluminescence in Aqueous Solution. *Chemosensors* **2022**, *10*, 174. [[CrossRef](#)]
47. Silva, J.P.; González-Berdullas, P.; Pereira, M.; Duarte, D.; Rodríguez-Borges, J.E.; Vale, N.; Esteves da Silva, J.C.G.; Pinto da Silva, L. Evaluation of the anticancer activity and chemiluminescence of a halogenated coelenterazine analog. *J. Photochem. Photobiol. A* **2023**, *434*, 114228. [[CrossRef](#)]
48. Sousa, J.; Magalhães, C.M.; González-Berdullas, P.; Esteves da Silva, J.C.G.; Pinto da Silva, L. Comparative Investigation of the Chemiluminescent Properties of a Dibrominated Coelenterazine Analog. *Int. J. Mol. Sci.* **2022**, *23*, 8490. [[CrossRef](#)]
49. Shimomura, O.; Teranishi, K. Light-emitters involved in the luminescence of coelenterazine. *Luminescence* **2000**, *15*, 51–58. [[CrossRef](#)]
50. Xiao, Y.F.; Chen, J.X.; Chen, W.C.; Zheng, X.; Cao, C.; Tan, J.; Cui, X.; Yuan, Z.; Ji, S.; Lu, G.; et al. Achieving high singlet-oxygen generation by applying the heavy-atom effect to thermally activated delayed fluorescent materials. *Chem. Commun.* **2021**, *57*, 4902–4905. [[CrossRef](#)]
51. Xiao, H.; Li, P.; Tang, B. Recent progresses in fluorescent probes for detection of polarity. *Coord. Chem. Rev.* **2021**, *427*, 213582. [[CrossRef](#)]
52. Qi, X.; Yang, X.; Du, L.; Li, M. Polarity-based fluorescence probes: Properties and applications. *RSC Med. Chem.* **2021**, *12*, 1826–1838.
53. Ma, C.; Sun, W.; Xu, L.; Qian, Y.; Dai, J.; Zhong, G.; Hou, Y.; Liu, J.; Shen, B. A minireview of viscosity-sensitive fluorescent probes: Design and biological applications. *J. Mater. Chem. B* **2020**, *8*, 9642–9651. [[CrossRef](#)] [[PubMed](#)]
54. Furstenberg, A. Water in Biomolecular Fluorescence Spectroscopy and Imaging: Side Effects and Remedies. *Chimia* **2017**, *71*, 26–31. [[CrossRef](#)] [[PubMed](#)]
55. Maillard, J.; Klehs, K.; Rumble, C.; Vauthey, E.; Heilemann, M.; Furstenberg, A. Universal quenching of common fluorescent probes by water and alcohols. *Chem. Sci.* **2021**, *12*, 1352–1362. [[CrossRef](#)] [[PubMed](#)]
56. Liu, Y.C.; Lu, G.D.; Zhou, J.H.; Rong, J.W.; Liu, H.Y.; Wang, H.Y. Fluoranthene dyes for the detection of water content in methanol. *RSC Adv.* **2022**, *12*, 7405–7412. [[CrossRef](#)]
57. Lu, T.; Chen, F. Multiwfn: A multifunctional wavefunction analyzer. *J. Comput. Chem.* **2012**, *33*, 580–592. [[CrossRef](#)]
58. Cardoso, I.M.F.; Cardoso, R.M.F.; Pinto da Silva, L.; Esteves da Silva, J.C.G. UV-Based Advanced Oxidation Processes of Remazol Brilliant Blue R Dye Catalyzed by Carbon Dots. *Nanomaterials* **2022**, *12*, 2116. [[CrossRef](#)]
59. Brouwer, A.M. Standards for photoluminescence quantum yield measurements in solution (IUPAC technical report). *Pure Appl. Chem.* **2011**, *83*, 2213–2228. [[CrossRef](#)]
60. Orge, B.; Rodríguez, A.; Canosa, J.M.; Marino, G.; Iglesias, M.; Tojo, J. Variation of densities, refractive indices, and speeds of sound with temperature of methanol or ethanol with hexane, heptane, and octane. *J. Chem. Eng. Data* **1999**, *44*, 1041–1047. [[CrossRef](#)]
61. Herráez, J.V.; Belda, R. Refractive indices, densities and excess molar volumes of monoalcohols + water. *J. Solut. Chem.* **2006**, *35*, 1315–1328. [[CrossRef](#)]
62. Ripin, A.; Mudalip, S.K.A.; Yunus, R.M. Effects of Ultrasonic Waves on Enhancement of Relative Volatilities in Methanol–Water Mixtures. *J. Teknol.* **2012**, *48*, 61–73. [[CrossRef](#)]
63. Chai, J.D.; Head-Gordon, M. Long-range corrected hybrid density functionals with damped atom-atom dispersion corrections. *Phys. Chem. Chem. Phys.* **2008**, *10*, 6615–6620. [[CrossRef](#)] [[PubMed](#)]
64. Adamo, C.; Jacquemin, D. The calculations of excited-state properties with time-dependent density functional theory. *Chem. Soc. Rev.* **2013**, *42*, 845–856. [[CrossRef](#)] [[PubMed](#)]
65. Yanai, T.; Tew, D.; Handy, N. A new hybrid exchange-correlation functional using the Coulomb-attenuating method (CAM-B3LYP). *Chem. Phys. Lett.* **2004**, *393*, 51–57. [[CrossRef](#)]
66. Adamo, C.; Barone, V. Toward reliable density functional methods without adjustable parameters: The PBE0 model. *J. Chem. Phys.* **1999**, *110*, 6158–6169. [[CrossRef](#)]
67. Frisch, M.J.; Trucks, G.W.; Schlegel, H.B.; Scuseria, G.E.; Robb, M.A.; Cheeseman, J.R.; Scalmani, G.; Barone, V.; Petersson, G.A.; Nakatsuji, H.; et al. *Gaussian 09, Revision D.01*; Gaussian, Inc.: Wallingford, CT, USA, 2016.